

Stiffness Analysis of a Planar 3-RPS Parallel Manipulator

Bo Hu, Chunxiao Song and Bo Li

Abstract This paper studied the stiffness model and characteristics of a planar 3-RPS PM with 3-DOF. The 6×6 form stiffness matrix of the planar 3-RPS PM is derived with both active and constrained wrenches considered. To characteristic the stiffness of the planer 3-RPS PM, two decomposition methods including the eigenscrew decomposition and the principle axes decomposition are applied to the stiffness matrix. The stiffness matrix decomposition provides a physical interpretation and allows the identification of the compliant axes of the planar 3-RPS PM.

Keywords Planar parallel manipulator · Stiffness · Eigenscrew decomposition · Principle axes decomposition · Compliant aixs

1 Introduction

In recent years, the planar 3 degree of freedom (DOF) parallel manipulators (PMs) have attracted much attention (Angeles 2014). Merlet et al. (1998) presented some definitions such as constant orientation workspace, reachable workspace and dexterous workspace for the planar PMs. Binaud et al. (2010) compared the sensibility of five 3-DOF planar PMs including the 3-RPR, 3-RPR, 3-RRR, 3-RRR and 3-PRR PMs. Mejia et al. (2015) derived a mathematical closed-form solution to obtain the maximum force with a prescribed moment in 3-DOF planar mechanisms. Kucuk (2009) performed dexterity comparison for seven 3-DOF planar PMs with two kinematic chains using genetic algorithms and indicated that the PPR planar

B. Hu (✉) · C. Song · B. Li

Parallel Robot and Mechatronic System Laboratory of Hebei Province,
Yanshan University, Qinhuangdao 066004, Hebei, China
e-mail: hubo@ysu.edu.cn

B. Hu · C. Song · B. Li

Key Laboratory of Advanced Forging and Stamping Technology and Science
of Ministry of National Education, Yanshan University,
Qinhuangdao 066004, Hebei, China

© Springer International Publishing Switzerland 2017

D. Zhang and B. Wei (eds.), *Mechatronics and Robotics Engineering for Advanced and Intelligent Manufacturing*, Lecture Notes in Mechanical Engineering, DOI 10.1007/978-3-319-33581-0_2

robot manipulator is the best configuration with the best dexterous maneuverability among the others. Dong et al. (2016) proposed a piezoelectric actuated 3-RPR planar micro-manipulator with orthogonal structure and developed its prototype.

Stiffness analysis plays an important role in design of planar 3-DOF PMs. In this aspect, Gosselin (1990) derived general $n \times n$ stiffness matrix for n -DOF PMs by only considering the elastic deformation of actuator factor. Wu et al. (2010) compared the stiffness performance of 4-RRR, 3-RRR and 2-RRR PMs. Zhao et al. (2007) investigated the stiffness performance of planar parallel 3-RRR mechanism with flexible joints.

Most of the stiffness model of planar PMs only considered the actuator factor while the constraint factors were not considered. Recently, the stiffness model considered both active and constrained wrenches has been established for various spatial lower mobility PMs (Li and Xu 2008; Hu and Lu 2011; Hu et al. 2014). Due to the consideration of constraints, this stiffness model is more suitable for the lower mobility PMs. However, up to now, the stiffness models of planar PMs with both active and constrained wrenches considered have not been studied.

Stiffness characteristic analysis is also an important research content for the planar PMs. To investigate the stiffness characteristics of PMs, some researchers proposed effective approaches for the stiffness matrix decomposition (Loncaric 1987; Huang and Schimmels 2000; Chen et al. 2015). Huang and Schimmels (2000) proposed an alternative synthesis algorithm for realization of an arbitrary spatial stiffness matrices, which has been widely used in stiffness characteristic analysis. Chen et al. (2015) presented an alternative decomposition of stiffness matrices, which can be used in both Plucker's ray and axis coordinates. And the compliant axis proposed by Patterson and Lipkin (1993a) is also a better way to explain the characteristic of stiffness.

For the above reasons, the stiffness model and characteristic of a novel planar 3-RPS PM which have constrained forces is studied in this paper.

2 Stiffness Model of the Planar 3-RPS PM

2.1 Kinematics Description

The planar 3-RPS PM includes a base B , a moving platform m , three identical RPS (revolute joint-active prismatic joint-spherical joint)-type leg. Here, B is a regular triangle with O as its center and A_i ($i = 1, 2, 3$) as its three vertices. m is a regular triangle with o as its center and a_i ($i = 1, 2, 3$) as its three vertices. For the planar 3-RPS PM, the three R joints are perpendicular with B (see Fig. 1).

Let \perp be a perpendicular constraint and \parallel be a parallel constraint. Let $\{B\}$ be a frame O -XYZ attached on B at O , $\{m\}$ be a frame o -xyz attached on m at o . Some geometrical conditions ($X \parallel A_1A_3$, $Y \perp A_1A_3$, $Z \perp B$, $x \parallel a_1a_3$, $y \perp a_1a_3$, $z \perp m$) for O -XYZ and o -xyz are satisfied.

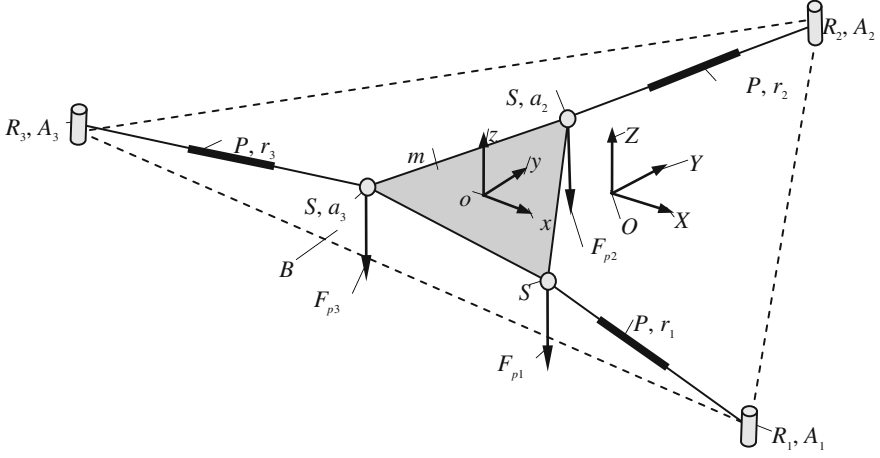


Fig. 1 Sketch of the planar 3-RPS PM

For the planar 3-RPS PM, the unit vectors \mathbf{R}_i of R_i ($i = 1, 2, 3$) in $\{B\}$ can be expressed as following:

$$\mathbf{R}_1 = \mathbf{R}_2 = \mathbf{R}_3 = \begin{bmatrix} 0 \\ 0 \\ 1 \end{bmatrix} \quad (1)$$

The position vectors \mathbf{A}_i ($i = 1, 2, 3$) of three vertices A_i in $\{B\}$ can be expressed as follows:

$$\mathbf{A}_1 = \frac{1}{2} \begin{bmatrix} qL \\ -L \\ 0 \end{bmatrix}, \quad \mathbf{A}_2 = \begin{bmatrix} 0 \\ L \\ 0 \end{bmatrix}, \quad \mathbf{A}_3 = -\frac{1}{2} \begin{bmatrix} qL \\ L \\ 0 \end{bmatrix}, \quad q = \sqrt{3}, \quad (2a)$$

where, L denotes the distance from the center of O to A_i .

The coordinate a_i ($i = 1, 2, 3$) in $\{m\}$ can be expressed as following:

$${}^m\mathbf{a}_1 = \frac{1}{2} \begin{bmatrix} ql \\ -l \\ 0 \end{bmatrix}, \quad {}^m\mathbf{a}_2 = \begin{bmatrix} 0 \\ l \\ 0 \end{bmatrix}, \quad {}^m\mathbf{a}_3 = -\frac{1}{2} \begin{bmatrix} ql \\ l \\ 0 \end{bmatrix} \quad (2b)$$

where, l denotes the distance from the center of o to a_i .

The coordinate a_i in $\{B\}$ can be expressed as following:

$${}^B\mathbf{a}_i = \begin{bmatrix} X_{ai} \\ Y_{ai} \\ Z_{ai} \end{bmatrix} = {}^B_m\mathbf{R} {}^m\mathbf{a}_i + \mathbf{o}, \quad {}^B_m\mathbf{R} = \begin{bmatrix} c_\alpha & -s_\alpha & 0 \\ s_\alpha & c_\alpha & 0 \\ 0 & 0 & 1 \end{bmatrix}, \quad {}^B\mathbf{o} = \begin{bmatrix} X_o \\ Y_o \\ Z_o \end{bmatrix} \quad (2c)$$

Here, α denotes the angle between B and m .

From Eqs. (2a), (2b) and (2c), the inverse solution can be formulated as following:

$$\begin{aligned} r_1^2 &= (qlc_\alpha/2 + ls_\alpha/2 + X_o - qL/2)^2 + (qls_\alpha/2 - lc_\alpha/2 + Y_o + L/2)^2 \\ r_2^2 &= (-ls_\alpha + X_o)^2 + (lc_\alpha + Y_o - L)^2 \\ r_3^2 &= (-qlc_\alpha/2 + ls_\alpha/2 + X_o + qL/2)^2 + (-qls_\alpha/2 - lc_\alpha/2 + Y_o - L)^2 \end{aligned} \quad (3)$$

Here r_i ($i = 1, 2, 3$) is the length of i th leg.

Based on the geometrical approach for determining the constrained forces/torques (Hu et al. 2014), one constrained force F_{pi} ($i = 1, 2, 3$) which is parallel with R_i and passes through the center of S joint in each RPS type leg can be determined.

As the constrained forces/torques do not work to m , it leads to

$$\begin{bmatrix} \mathbf{Z}^T & (\mathbf{d}_i \times \mathbf{Z})^T \end{bmatrix} \begin{bmatrix} \mathbf{v} \\ \boldsymbol{\omega} \end{bmatrix} = 0, \quad \mathbf{Z} = [0 \quad 0 \quad 1]^T, \quad \mathbf{d}_i = \mathbf{a}_i - \mathbf{o} \quad (4a)$$

where, \mathbf{f}_i denotes the unit vector of F_{pi} , \mathbf{a}_i ($i = 1, 2, 3$) and \mathbf{o} denote the coordinates of \mathbf{a}_i and \mathbf{o} respect to O , respectively.

From Eq. (4a) and Hu et al. (2014), it leads to

$$\mathbf{V}_r = \mathbf{J}_{6 \times 6} \begin{bmatrix} \mathbf{v} \\ \boldsymbol{\omega} \end{bmatrix}, \quad \mathbf{J}_{6 \times 6} = \begin{bmatrix} \boldsymbol{\delta}_1^T & (\mathbf{d}_1 \times \boldsymbol{\delta}_1)^T \\ \boldsymbol{\delta}_2^T & (\mathbf{d}_2 \times \boldsymbol{\delta}_2)^T \\ \boldsymbol{\delta}_3^T & (\mathbf{d}_3 \times \boldsymbol{\delta}_3)^T \\ \mathbf{Z}^T & (\mathbf{d}_1 \times \mathbf{Z})^T \\ \mathbf{Z}^T & (\mathbf{d}_2 \times \mathbf{Z})^T \\ \mathbf{Z}^T & (\mathbf{d}_3 \times \mathbf{Z})^T \end{bmatrix}, \quad \mathbf{V}_r = \begin{bmatrix} v_{r1} \\ v_{r2} \\ v_{r3} \\ 0 \\ 0 \\ 0 \end{bmatrix}, \quad \boldsymbol{\delta}_i = \frac{\mathbf{a}_i - \mathbf{A}_i}{|\mathbf{a}_i - \mathbf{A}_i|} \quad (4b)$$

Here, \mathbf{v} and $\boldsymbol{\omega}$ denote the linear and angular velocities of m , respectively, and $\mathbf{J}_{6 \times 6}$ is the Jacobian matrix of the planar 3-RPS PM.

2.2 Stiffness Matrix Establishment

Let $\mathbf{F}_o = [F_x \ F_y \ F_z]^T$ and $\mathbf{T}_o = [T_x \ T_y \ T_z]^T$ be the forces and torques applied on m at o , respectively. Let F_{ri} and F_{pi} ($i = 1, 2, 3$) be the active force and constrained force of r_i , respectively. Using the principle of virtual work, we obtain

$$\mathbf{F}_r^T \mathbf{V}_r + [\mathbf{F}_o^T \quad \mathbf{T}_o^T] \begin{bmatrix} \mathbf{v} \\ \boldsymbol{\omega} \end{bmatrix} = 0 \quad (5a)$$

Here, $\mathbf{F}_r = [F_{r1} \ F_{r2} \ F_{r3} \ F_{p1} \ F_{p2} \ F_{p3}]^T$.

From Eqs. (4b) and (5a), it leads to

$$\mathbf{F}_r = -(\mathbf{J}_{6 \times 6}^{-1})^T \begin{bmatrix} \mathbf{F}_o \\ \mathbf{T}_o \end{bmatrix}, \begin{bmatrix} \mathbf{F}_o \\ \mathbf{T}_o \end{bmatrix} = \mathbf{J}_{6 \times 6}^T \mathbf{F}_r \quad (5b)$$

In the RPS type leg, the active force F_{ri} ($i = 1, 2, 3$) produces a flexibility deformations along r_i and the constrained force F_{pi} ($i = 1, 2, 3$) produces a bending deformation which is perpendicular with r_i .

Let δr_i ($i = 1, 2, 3$) denotes the flexibility deformations along r_i produced by the active force F_{ri} , it leads to

$$F_{ri} = k_{ri} \delta r_i, \quad k_{ri} = \frac{ES_i}{r_i} \quad (6a)$$

Here, E is the modular of elasticity and S_i denotes the i th leg's cross section of RPS type leg.

Let δd_i ($i = 1, 2, 3$) denotes the bending deformation of r_i produced by the constrained forces F_{pi} . It leads to,

$$F_{pi} = k_{pi} \delta d_i, \quad k_{pi} = \frac{3EI}{r_i^3} \quad (6b)$$

where, I is the moment of inertia.

From Eqs. (6a) and (6b), it leads to

$$\mathbf{F}_r = \mathbf{K}_p \begin{bmatrix} \delta \mathbf{r} \\ \delta \mathbf{d} \end{bmatrix}, \quad \delta \mathbf{r} = \begin{bmatrix} \delta r_1 \\ \delta r_2 \\ \delta r_3 \end{bmatrix}, \quad \delta \mathbf{d} = \begin{bmatrix} \delta d_1 \\ \delta d_2 \\ \delta d_3 \end{bmatrix}, \quad (7)$$

$$\mathbf{K}_p = \begin{bmatrix} k_{r1} & 0 & 0 & 0 & 0 & 0 \\ 0 & k_{r2} & 0 & 0 & 0 & 0 \\ 0 & 0 & k_{r3} & 0 & 0 & 0 \\ 0 & 0 & 0 & k_{p1} & 0 & 0 \\ 0 & 0 & 0 & 0 & k_{p2} & 0 \\ 0 & 0 & 0 & 0 & 0 & k_{p3} \end{bmatrix}$$

Let $\delta \mathbf{p}$ and $\delta \boldsymbol{\Phi}$ be the position and orientation deformation of m , respectively. By using the principle of virtual work, the following equation can be derived:

$$\mathbf{F}_r^T \begin{bmatrix} \delta \mathbf{r} \\ \delta \mathbf{d} \end{bmatrix} = - \begin{bmatrix} \mathbf{F}_o^T & \mathbf{T}_o^T \end{bmatrix} \begin{bmatrix} \delta \mathbf{p} \\ \delta \Phi \end{bmatrix} \quad (8)$$

From Eqs. (5b), (7) and (8), it leads to

$$\begin{bmatrix} \mathbf{F}_o \\ \mathbf{T}_o \end{bmatrix} = \mathbf{K} \begin{bmatrix} \delta \mathbf{p} \\ \delta \Phi \end{bmatrix}, \quad \mathbf{K} = \mathbf{J}_{6 \times 6}^T \mathbf{K}_p \mathbf{J}_{6 \times 6} \quad (9)$$

Here, \mathbf{K} is the stiffness matrix of the planar 3-RPS PM.

3 Stiffness Characteristics Analysis

To characteristic the stiffness of the planer 3-RPS PM, the eigenscrew decomposition and the principle axes decomposition approaches are applied to the stiffness matrix. Loncaric (1987) proposed that by using the decomposition, the stiffness matrix can be realized by several parallel simple or screw springs, which is a direct correspondence between the mechanism realization and physical appreciation of a spatial stiffness matrix. In addition, the compliant axis of the planer 3-RPS PM are also studied in this section to reversal the characteristic of this PM.

3.1 The Eigenscrew Decomposition of Stiffness Matrix

The eigenscrew problem mentioned by Patterson and Lipkin (1993a) of the spatial stiffness matrix can be expressed as following:

$$\mathbf{K} \Delta \mathbf{e} = \lambda \mathbf{e} \quad (10)$$

where λ and the corresponding \mathbf{e} are the eigenvalue and eigenvector of $\mathbf{K} \Delta$, respectively. The transformation matrix Δ interchanges the first and last three components of a screw, which can be expressed as following:

$$\Delta = \begin{bmatrix} \mathbf{0}_{3 \times 3} & \mathbf{I}_{3 \times 3} \\ \mathbf{I}_{3 \times 3} & \mathbf{0}_{3 \times 3} \end{bmatrix} \quad (11)$$

The eigenscrew decomposition proposed by Huang and Schimmels (2000) of spatial stiffness matrix can be expressed as:

$$\mathbf{K} = \sum_{i=1}^6 k_i \mathbf{w}_i \mathbf{w}_i^T, \quad k_i = \frac{\lambda_i}{2h_i}, \quad h_i = \frac{1}{2} \mathbf{w}_i^T \Delta \mathbf{w}_i \quad (12)$$

where, spring wrench \mathbf{w}_i is the unitization of \mathbf{e}_i ($i = 1, \dots, 6$), h_i is the pitch of \mathbf{w}_i and \mathbf{w}_i can be defined as:

$$\mathbf{w}_i = \begin{bmatrix} \mathbf{n}_i \\ \boldsymbol{\rho}_i \times \mathbf{n}_i + h_i \mathbf{n}_i \end{bmatrix} \quad (13)$$

Here, \mathbf{n}_i and $\boldsymbol{\rho}_i$ ($i = 1, \dots, 6$) are the direction and position vectors of the i th spring, respectively.

3.2 The Principle Axes Decomposition of Spatial Stiffness Matrix

In the principle axes decomposition (Chen et al. 2015), the wrench $\underline{\mathbf{F}}$ and $\delta \underline{\mathbf{P}}$ are expressed in axis coordinate. The relation between ray and axis coordinate can be expressed as following:

$$\underline{\mathbf{F}} = \Delta \mathbf{F}, \quad \delta \underline{\mathbf{P}} = \Delta \delta \mathbf{P} \quad (14)$$

From Eq. (11), it leads to

$$\Delta \Delta = \mathbf{E} \quad (15)$$

here \mathbf{E} is an identity matrix.

The relation of stiffness matrices between these two systems can be derived from Eqs. (14) and (15) as following,

$$\underline{\mathbf{K}} = \Delta \mathbf{K} \Delta = \begin{bmatrix} \underline{\mathbf{A}} & \underline{\mathbf{B}} \\ \underline{\mathbf{B}}^T & \underline{\mathbf{C}} \end{bmatrix} \quad (16)$$

where the symmetric 3×3 block matrices $\underline{\mathbf{A}}$ and $\underline{\mathbf{C}}$ denote the rotational and translational parts, and $\underline{\mathbf{B}}$ denote the coupling part.

$\underline{\mathbf{K}}$ can be represented in a reduced form $\underline{\mathbf{K}}_O$ by applying a pure rotation $\mathbf{R} = \mathbf{Q}^T$ to the current frame in order to translate $\underline{\mathbf{C}}$ to a diagonal form $\underline{\mathbf{C}}_O$, where \mathbf{Q} represents a 3×3 orthogonal matrix whose columns are just the eigenvectors of $\underline{\mathbf{C}}$. Then the stiffness matrix can be decomposed into two sets of rank-1 symmetric stiffness matrices as following (Chen et al. 2015):

$$\begin{aligned} \underline{\mathbf{K}}_O &= \begin{bmatrix} \underline{\mathbf{A}}_O & \underline{\mathbf{B}}_O \\ \underline{\mathbf{B}}_O^T & \underline{\mathbf{C}}_O \end{bmatrix} = \underline{\mathbf{K}}_{OS} + \underline{\mathbf{K}}_{OT} = \sum_{i=1}^3 k_i \mathbf{w}_i \mathbf{w}_i^T + \sum_{j=4}^6 k_j \mathbf{w}_j \mathbf{w}_j^T, \\ \underline{\mathbf{A}}_O &= \mathbf{Q}^T \underline{\mathbf{A}} \mathbf{Q}, \quad \underline{\mathbf{B}}_O = \mathbf{Q}^T \underline{\mathbf{B}} \mathbf{Q}, \quad \underline{\mathbf{A}}_{OT} = \underline{\mathbf{A}}_O - \underline{\mathbf{B}}_O \underline{\mathbf{C}}_O^{-1} \underline{\mathbf{B}}_O^T, \\ \mathbf{w}_i &= \begin{bmatrix} \frac{1}{k_i} \mathbf{b}_i^T & \mathbf{e}_i^T \end{bmatrix}^T, \quad \mathbf{w}_j = \begin{bmatrix} \boldsymbol{\alpha}_i^T & \mathbf{0}_{3 \times 1}^T \end{bmatrix}^T, \end{aligned} \quad (17)$$

where, $\underline{\mathbf{K}}_{OS}$ and $\underline{\mathbf{K}}_{OT}$ are the principal components corresponding to the screw and torsional springs, respectively. k_i ($i = 1, 2, 3$) and k_j ($j = 1, 2, 3$) are the i th eigenvalue of $\underline{\mathbf{C}}$ and $\underline{\mathbf{A}}_{OT}$, respectively. \mathbf{e}_i ($i = 1, 2, 3$) denotes the unit vector associated with the coordinate axis of $\{O\}$, namely $\mathbf{e}_1 = [1, 0, 0]^T$, $\mathbf{e}_2 = [0, 1, 0]^T$, $\mathbf{e}_3 = [0, 0, 1]^T$, \mathbf{b}_i represents the i th column of $\underline{\mathbf{B}}_O$, \mathbf{a}_i represents the i th eigenvector of $\underline{\mathbf{A}}_{OT}$, and \mathbf{w}_i ($i = 1, 2, 3$) is the i th wrench-compliant axis of this elastic system.

From Eq. (17), any spatial stiffness matrix can be uniquely realized by three screw and three torsional springs connected in parallel, and the screw springs and torsional springs are orthogonal to each other, respectively.

Let $\{C\}$ be a frame $C\text{-}X_QY_QZ_Q$ with the direction of X_Q , Y_Q and Z_Q -axis are along each row of $\underline{\mathbf{Q}}$, respectively. Then $\underline{\mathbf{K}}$ can be expressed in $\{C\}$ as following:

$$\underline{\mathbf{K}}_C = \begin{bmatrix} \underline{\mathbf{A}}_* & 0 \\ 0 & 0 \end{bmatrix} + \begin{bmatrix} \underline{\mathbf{B}}_*\underline{\mathbf{C}}\underline{\mathbf{B}}_* & \underline{\mathbf{B}}_*\underline{\mathbf{C}} \\ \underline{\mathbf{C}}\underline{\mathbf{B}}_* & \underline{\mathbf{C}} \end{bmatrix}, \quad (18)$$

$$\underline{\mathbf{A}}_* = \underline{\mathbf{A}} - \underline{\mathbf{B}}\underline{\mathbf{C}}^{-1}\underline{\mathbf{B}}^T, \quad \underline{\mathbf{B}}_* = \frac{1}{2}(\underline{\mathbf{B}}\underline{\mathbf{C}}^{-1} + \underline{\mathbf{C}}^{-1}\underline{\mathbf{B}}^T)$$

Equation (18) is referred to as the central principle frame, and C is also called the center of stiffness. $\underline{\mathbf{K}}_C$ is the simplest form of the spatial stiffness matrices, which decouples rotational and translational aspects of stiffness to a certain extent. In (18), there only exists three 3×3 symmetric blocks $\underline{\mathbf{A}}_*$, $\underline{\mathbf{B}}_*$, $\underline{\mathbf{C}}$, which correspond to the rotational, coupling and translational parts, respectively.

The homogeneous transformation matrix is given by,

$$g_K = \begin{bmatrix} \underline{\mathbf{Q}} & \mathbf{p} \\ \mathbf{0}_{3 \times 1}^T & 1 \end{bmatrix}, \quad \hat{\mathbf{p}} = \frac{1}{2}(\underline{\mathbf{B}}_O\underline{\mathbf{C}}^{-1} - \underline{\mathbf{C}}^{-1}\underline{\mathbf{B}}_O) \quad (19)$$

where \mathbf{p} is the coordinate of C respected to the original reference frame $\{B\}$.

Based on the above analysis, the stiffness matrix of planar 3-RPS PM can be decomposed into two sets of three rank-1 symmetric matrices, which can also identify the elastic system's force-deflection behavior of planar 3-RPS PM.

3.3 Compliant Axis and Center of Compliance

For a compliant axis (Patterson and Lipkin 1993b), a force produces a parallel liner deformation and a rotational deformation produces a parallel couple. The compliant axis exists if and only if there are two collinear eigenscrews with eigenvalues of equal magnitude and opposite sign. Thus, not all the elastic system exhibits compliant axes. Wrench-compliant and twist-compliant axes are the basic of a compliant axis hierarchy, and most elastic systems exhibit the wrench-compliant/twist-compliant axes. Wrench-compliant axis exists when a wrench produces a parallel linear deformation, and a twist-compliant axis exists when a twist produces a parallel couple. Such kinds of the force-deflection behavior can be interpreted as following:

$$\begin{bmatrix} \mathbf{f} \\ \boldsymbol{\rho} \times \mathbf{f} + h\mathbf{f} \end{bmatrix} = \mathbf{K}\Delta \begin{bmatrix} 0 \\ k_f \mathbf{f} \end{bmatrix}, \begin{bmatrix} 0 \\ k_\delta \boldsymbol{\theta} \end{bmatrix} = \mathbf{K}\Delta \begin{bmatrix} \boldsymbol{\theta} \\ \boldsymbol{\rho} \times \boldsymbol{\theta} + h\boldsymbol{\theta} \end{bmatrix} \quad (20)$$

where, \mathbf{f} is a force, $\boldsymbol{\theta}$ is a rotational deformation, k_f and k_δ are translational and rotational stiffness, h and $\boldsymbol{\rho}$ are the pitch and position vector of a wrench/twist, respectively.

If h is equal to 0, then Eq. (20) is turn into,

$$\begin{bmatrix} \mathbf{f} \\ \boldsymbol{\rho} \times \mathbf{f} \end{bmatrix} = \mathbf{K}\Delta \begin{bmatrix} 0 \\ k_f \mathbf{f} \end{bmatrix}, \quad \begin{bmatrix} 0 \\ k_\delta \boldsymbol{\theta} \end{bmatrix} = \mathbf{K}\Delta \begin{bmatrix} \boldsymbol{\theta} \\ \boldsymbol{\rho} \times \boldsymbol{\theta} \end{bmatrix} \quad (21)$$

Then the wrench-compliant and twist-compliant axes are turn into force-compliant and rotation-compliant axes, respectively.

If an elastic system has three linearly independent compliant axes and they intersect at the same point, then this point is called the center of compliance. The center of compliance refers to a very specialized concept. At this point, a force passes through the point produces a collinear translation, and a rotation through the point produces a collinear couple (Patterson and Lipkin 1993a). The planar 3-RPS PM has such a center of compliance, which is verified in the last section.

3.4 The Stiffness Characteristics Along Z-Axis

The Jacobian matrix in (4a), the stiffness matrix in (9) and \mathbf{K}_P can be divided into 4 parts, respectively

$$\mathbf{J} = \begin{bmatrix} \mathbf{J}_1 & \mathbf{J}_2 \\ \mathbf{J}_3 & \mathbf{J}_4 \end{bmatrix}, \quad \mathbf{K} = \begin{bmatrix} \mathbf{C} & \mathbf{B} \\ \mathbf{B}^T & \mathbf{A} \end{bmatrix}, \quad \mathbf{K}_P = \begin{bmatrix} \mathbf{K}_r & \mathbf{0} \\ \mathbf{0} & \mathbf{K}_p \end{bmatrix}, \quad (22)$$

$$\mathbf{K}_r = \begin{bmatrix} k_{r1} & 0 & 0 \\ 0 & k_{r2} & 0 \\ 0 & 0 & k_{r3} \end{bmatrix}, \quad \mathbf{K}_p = \begin{bmatrix} k_{p1} & 0 & 0 \\ 0 & k_{p2} & 0 \\ 0 & 0 & k_{p3} \end{bmatrix}$$

Here, \mathbf{J}_i ($i = 1, 2, 3, 4$) are 3×3 form matrices.

The relation of these blockings can be expressed as

$$\mathbf{C} = \mathbf{J}_1^T \mathbf{K}_r \mathbf{J}_1 + \mathbf{J}_3^T \mathbf{K}_p \mathbf{J}_3, \quad \mathbf{B} = \mathbf{J}_1^T \mathbf{K}_r \mathbf{J}_2 + \mathbf{J}_3^T \mathbf{K}_p \mathbf{J}_4, \quad (23)$$

$$\mathbf{A} = \mathbf{J}_2^T \mathbf{K}_r \mathbf{J}_2 + \mathbf{J}_4^T \mathbf{K}_p \mathbf{J}_4$$

The components of δ_i ($i = 1, 2, 3$) along Z-axis are 0, from Eq. (4b), the matrix \mathbf{C} can be expressed as

$$\mathbf{C} = \begin{bmatrix} k_{11} & k_{12} & 0 \\ k_{13} & k_{14} & 0 \\ 0 & 0 & k_{15} \end{bmatrix} \quad (24)$$

k_{1i} ($i = 1, 2$) is determined by \mathbf{J}_1 , k_{ri} and k_{pi} ($i = 1, 2, 3$). From Eq. (24), it can be seen that \mathbf{C} must have one eigenvalue k_{15} ($k_{15} = k_{p1} + k_{p2} + k_{p3}$), and the corresponding eigenvector is $[0 \ 0 \ 1]^T$, which is always along Z-axis.

From Eq. (16), the direction of a wrench-compliant axis is determined by the eigenvector of $\underline{\mathbf{C}}$, which is equal to \mathbf{C} in Eq. (22). Obviously, the planar 3-RPS PM always have a wrench-compliant axis along Z-axis. The pith is determined by $\underline{\mathbf{B}}$, which is determined by the configuration of the PM. However, we can certain that a force along Z-axis only produce a linear deformation and will not affect another directions. Then the planar 3-RPS PM has better operation in Z-axis.

4 Numerical Examples

In this section, a 3D assembly manipulator and the finite element (FE) model of the planar 3-RPS PM is established to verify the stiffness model obtained in Sect. 2. Then, one numerical example is provided to characterize the stiffness matrix of planar 3-RPS PM based on the eigenscrew decomposition and principle axes decomposition. In this process, the stiffness matrix is realized by six springs connected in parallel based on two methods, and the compliant axes are obtained through eigenscrew decomposition, which identified the decoupled stiffness matrix.

Set $X_0 = 0$ m, $Y_0 = 0$ m, $a = 10^\circ$, the corresponding length of legs are solved as: $r_1 = r_2 = r_3 = 0.8158$ m, and the stiffness matrix corresponding to this configuration is obtained as following:

$$\mathbf{K} = \begin{bmatrix} -2.7281 & -0.0000 & 0 & 0 & 0 & -0.0000 \\ -0.0000 & -2.7281 & 0 & 0 & 0 & 0.0000 \\ 0 & 0 & 0.0014 & 0.0000 & -0.0000 & 0 \\ 0 & 0 & 0.0000 & 0.0001 & 0.0000 & 0 \\ 0 & 0 & -0.0000 & 0.0000 & 0.0001 & 0.0000 \\ -0.0000 & 0.0000 & 0 & 0 & 0 & 0.0396 \end{bmatrix} \times 10^8 \quad (25)$$

4.1 Finite Element Analysis

In the Solid model of planar 3-RPS PM, S joint is constructed by three R joints (see Fig. 2). Assume a force $\mathbf{F}_o = [-20 \ -30 \ -60]^T$ N applied on the center of m . The simulated results based on finite element model for the deformation of m are

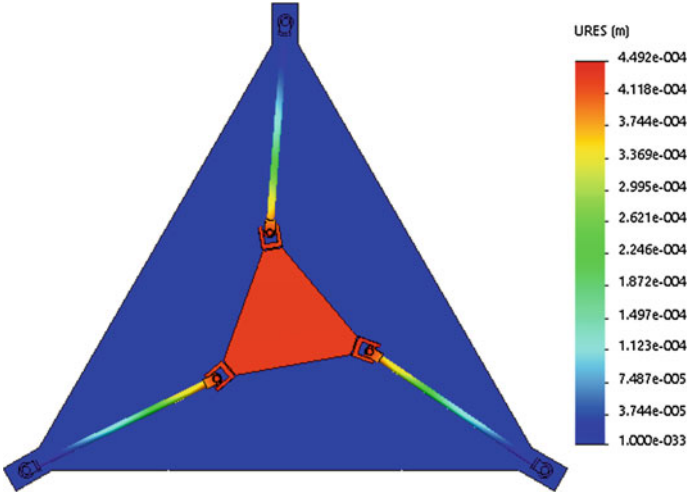


Fig. 2 The simulated result of 3-RPS PM

Table 1 The simulated results based on the finite element model and the theoretical results based on the stiffness model of the deformation of m

The deformation of m (mm)			Error rate (%)
	FE model	Stiffness model	
δx	-7.157×10^{-5}	-7.331×10^{-5}	2.3
δy	-1.113×10^{-4}	-1.110×10^{-4}	0.27
δz	-0.4298	-0.4337	0.89

derived as shown in Fig. 2. The simulated results based on the FE model and the calculated results based on the stiffness model are listed in Table 1.

From Table 1, we can see that the simulated results of FE model are almost equal to the calculated results of the stiffness model. The most error rate is 2.3 %, which is less than 3 %. Then, the FE model verify the correctness of the stiffness model. We also find that the deformation of m in Z-axis is approximate 10^4 times of the deformation in X-axis and Y-axis, which means a small external force in Z-axis would cause relatively large deformation in Z-axis, and this situation has not been mentioned in stiffness analyses of planar PMs in most of previous works. The stiffness model established in this paper presents this situation, which is also appropriate to other planar PMs.

4.2 Decomposition of Planar 3-RPS PM Stiffness Matrix

Applying the eigenscrew decomposition to the stiffness matrix (25), the corresponding six eigenvalue values λ , screw pitches h and the corresponding

Table 2 Parameters of springs based on the eigenscrew decomposition

Spring	k_i	\mathbf{n}_i	$\boldsymbol{\rho}_i$	h_i
1	1.3640×10^8	$[0, 1, 0]^T$	$[0, 0, 0]^T$	0.0055
2	1.3640×10^8	$[0, 1, 0]^T$	$[0, 0, 0]^T$	-0.0055
3	1.3640×10^8	$[1, 0, 0]^T$	$[0, 0, 0]^T$	0.0055
4	1.3640×10^8	$[1, 0, 0]^T$	$[0, 0, 0]^T$	-0.0055
5	6.9176×10^4	$[0, 0, 1]^T$	$[0, 0, 0]^T$	5.3470
6	6.9176×10^4	$[0, 0, -1]^T$	$[0, 0, 0]^T$	-5.3470

eigenscrews \mathbf{w} can be obtained by solving Eq. (12) and the results are shown in Eq. (26) as following:

$$\begin{aligned}
 \lambda &= \text{diag}([1.5049 \quad -1.5049 \quad 1.5049 \quad -1.5049 \quad -0.7398 \quad -0.7398]) \times 10^6 \\
 h &= \text{diag}([0.0055 \quad -0.0055 \quad 0.0055 \quad -0.0055 \quad -5.3470 \quad -5.3470]) \\
 \mathbf{w} &= \begin{bmatrix} 0 & 0 & 1 & 1 & 0 & 0 \\ 1 & 1 & 0 & 0 & 0 & 0 \\ 0 & 0 & 0 & 0 & 1 & 1 \\ 0 & 0 & -0.0055 & 0.0055 & 0 & 0 \\ 0.0055 & -0.0055 & 0 & 0 & 0 & 0 \\ 0 & 0 & 0 & 0 & 5.3470 & -5.3470 \end{bmatrix} \quad (26)
 \end{aligned}$$

The parameters of springs based on the eigenscrew decomposition are illustrated in Table 2.

Applying the principle axes decomposition to the stiffness matrix in Eq. (25), the central principal aspects of this spatial stiffness can then be obtained readily and given by,

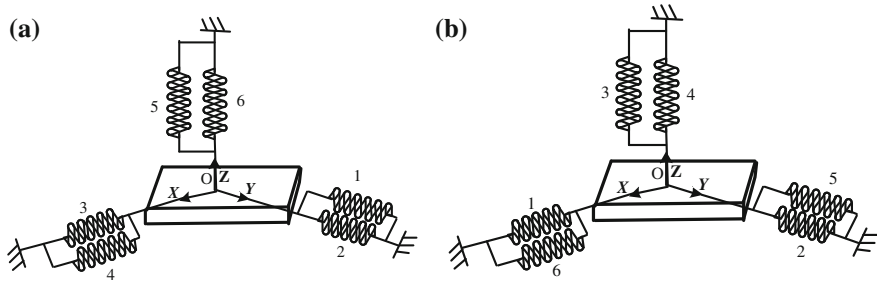
$$\begin{aligned}
 \underline{\mathbf{A}}_* &= \begin{bmatrix} 0.0083 & 0 & 0 \\ 0 & 0.0083 & 0 \\ 0 & 0 & 3.9556 \end{bmatrix} \times 10^6, \quad \underline{\mathbf{B}}_* = \begin{bmatrix} 0 & 0 & 0.0741 \\ 0 & 0 & -0.1672 \\ 0.0741 & -0.1672 & 0 \end{bmatrix} \times 10^{-10} \\
 \underline{\mathbf{C}}_* &= \begin{bmatrix} 2.7281 & 0 & 0 \\ 0 & 2.7281 & 0 \\ 0 & 0 & 0.0014 \end{bmatrix} \times 10^8 \quad (27)
 \end{aligned}$$

The corresponding homogeneous transformation matrix is given by,

$$\mathbf{g}_K = \begin{bmatrix} 1 & 0 & 0 & 0 \\ 0 & 1 & 0 & 0 \\ 0 & 0 & 1 & 0 \\ 0 & 0 & 0 & 1 \end{bmatrix} \quad (28)$$

Table 3 Parameters of springs based on the principle axes decomposition

Spring	k_i	\mathbf{n}_i	$\mathbf{\rho}_i$	h_i
1	2.7281×10^8	$[1, 0, 0]^T$	$[0, 0, 0]^T$	0
2	2.7281×10^8	$[0, 1, 0]^T$	$[0, 0, 0]^T$	0
3	1.3835×10^5	$[0, 0, 1]^T$	$[0, 0, 0]^T$	0
4	3.9555×10^6	$[0, 0, 1]^T$	/	∞
5	8.3012×10^3	$[0, 0, 1]^T$	/	∞
6	8.3012×10^3	$[0, 1, 0]^T$	/	∞

**Fig. 3** Physical interpretation of the stiffness matrix based on the eigenscrew decomposition (a) and principle axes decomposition (b)

In Eq. (27), $\underline{\mathbf{C}}_*$ is a diagonal matrix and the coupling matrix $\underline{\mathbf{B}}$ is turn into a symmetric matrix $\underline{\mathbf{B}}_*$, which is almost equal to null matrix.

The parameters of springs based on the principle axes decomposition are illustrated in Table 3.

The physical interpretation of this stiffness matrix realized by springs based on the eigenscrew decomposition and the principle axes decomposition are shown in Fig. 3a, b.

4.3 Compliant Axes of Planar 3-RPS PM

It can be seen from Fig. 3a that the stiffness matrix is realized by six screw springs. The six screw springs intersect at the coordinate center O . They can be divided into three groups, and each group has two springs. These two springs in each group are collinear and have the same stiffness constants, while opposite in sign. These three group springs are three compliant axes actually, which means the force and deformation about the compliant axes would not affect any other directions. These compliant axes can be expressed as following:

$$\mathbf{w}_c = \begin{bmatrix} 0 & 1 & 0 & 0 & 0.0055 & 0 \\ 1 & 0 & 0 & 0.0055 & 0 & 0 \\ 0 & 0 & 1 & 0 & 0 & 5.3470 \end{bmatrix}^T \quad (29)$$

From Eq. (29), it can be seen that the three compliants are orthogonality and along the direction of Y -, X -, Z -axes, respectively. The three compliant axes also intersect at the same point O , which means that the O is the center of the compliance of the elastic system. It also can be observed that the stiffness matrix is diagonal, which means the stiffness is decoupled in this configuration. In this situation, the stiffness matrix is identify with Class 3b presented by Patterson and Lipkin (1993b). In Class 3b, the elastic system has a pencil of compliant axes and a single compliant axis perpendicular to the pencil. Since $\lambda_1 = \lambda_3$, $h_1 = h_3$, and the eigenscrews corresponding to λ_1 and λ_3 are distributed in X - Y plane, it means that in the X - Y plane, a force (rotational deformation) through the origin produces a linear deformation(couple) parallel to the X - Y plane, and such kind of the force-deflection behavior can be interpreted by

$$\begin{aligned} [F_x \ F_y \ 0 \ 0 \ 0 \ 0] &= \lambda_i \mathbf{K} \Delta [0 \ 0 \ 0 \ F_x \ F_y \ 0], \\ [0 \ 0 \ 0 \ \delta\Phi_x \ \delta\Phi_y \ 0] &= \lambda_i \mathbf{K} \Delta [\delta\Phi_x \ \delta\Phi_y \ 0 \ 0 \ 0 \ 0], (i = 1, 3) \end{aligned}$$

In Table 3, the pitches of the first three springs are equal to 0. There are three force-compliant axes which are correspond with Eq. (29), they can be expressed as follow:

$$\mathbf{w} = \begin{bmatrix} 0 & 1 & 0 & 0 & 0 & 0 \\ 1 & 0 & 0 & 0 & 0 & 0 \\ 0 & 0 & 1 & 0 & 0 & 0 \end{bmatrix}^T \quad (30)$$

From Fig. 3b, it can be seen that the stiffness matrix is realized by six simple springs. The first three springs are perpendicularity mutually and intersect at O . The last three springs are perpendicularity mutually and intersect at O , and O is also the center of stiffness of this elastic system. In this configuration, the center of stiffness is degenerate to the center of compliance, which verifies the decoupled characteristic of the stiffness matrix in another way. There are four springs in the X - Y plane and two springs along the Z -axis, which is in accordance with the distribution of screw springs displayed in Fig. 3a. The three pitches of the first three springs are equal to 0, which means the three wrench-compliant axes degenerate to three force-compliant axes. The third spring is along Z -axis which indicated that a force act along Z -axis on the elastic system always only produce a collinear deformation.

5 Conclusions

The main contribution of this paper consists in analyzing the forces/torque situation, deformation and stiffness by considering active forces and constrained torques factors for the planar 3-RPS PM. By considering the constrained forces in each RPS leg, a 6×6 form Jacobian matrix is derived for a planar 3-RPS PM. This 6×6 form Jacobian matrix is used in the stiffness model which leads to a 6×6 form stiffness matrix.

A FE model is established to verify the stiffness model presented in this paper and the comparison results show that the stiffness model is applicable to such kind of planar PMs. And the results also show that the stiffness in Z-axis is much larger than X-axis and Y-axis which cannot be ignored in practical application.

A numeral example is analyzed to reveal the stiffness characteristic of the planar 3-RPS PM by eigenscrew decomposition and principle axes decomposition. The three compliant axes obtained by eigenscrew decomposition show that the stiffness matrix is decoupled in X-Y plane. And the compliant axis along Z-axis obtained by eigenscrew decomposition and the force-deformation axis along Z-axis obtained by principle axes decomposition show that a force act along Z-axis on the elastic system always only produce a collinear deformation without affect another direction.

The stiffness analysis modeling of the planar 3-RPS PM in this paper is fit for other planar PMs. This research provides a good reference for the stiffness analysis of the planar PMs.

References

- Angeles, J. (2014). *Fundamentals of robotic mechanical systems*. Springer.
- Binaud, N., Caro, S., & Wenger, P. (2010). Sensitivity comparison of planar parallel manipulators. *Mechanism and Machine Theory*, 45(11), 1477–1490.
- Chen, G. L., Wang, H., Lin, Z. Q., et al. (2015). The principle axes decomposition of spatial stiffness matrices. *IEEE Transactions on Robotics*, 31(1), 191–207.
- Dong, Y., Gao, F., & Yue, Y. (2016). Modeling and experimental study of a novel 3-RPR parallel micro-manipulator. *Robotics and Computer-Integrated Manufacturing*, 37, 115–124.
- Gosselin, C. M. (1990). Stiffness mapping for parallel manipulators. *IEEE Transactions on Robotics and Automation*, b3, 6, 377–382.
- Hu, B., & Lu, Y. (2011). Solving stiffness and deformation of a 3-UPU parallel manipulator with one translation and two rotations. *Robotica*, 29(6), 815–822.
- Hu, B., Mao, B., et al. (2014). Unified stiffness model of lower mobility parallel manipulators with linear active legs. *International Journal of Robotics and Automation*, 29(1), 58–66.
- Huang, S., & Schimmels, J. M. (2000). The eigenscrew decomposition of spatial stiffness matrices. *IEEE Transaction on Robotics and Automation*, 16(2), 146–156.
- Kucuk, S. (2009). A dexterity comparison for 3-DOF planar parallel manipulators with two kinematic chains using genetic algorithms. *Mechatronics*, 19(6), 868–877.
- Li, Y., & Xu, Q. (2008). Stiffness analysis for a 3-PUU parallel kinematic machine. *Mechanism and Machine Theory*, 43(2), 186–200.

- Loncaric, J. (1987). Normal forms of stiffness and compliance matrices. *IEEE Journal of Robotics and Automation*, 3(6), 567–572.
- Mejia, L., Simas, H., & Martins, D. (2015). Force capability in general 3 DoF planar mechanisms. *Mechanism and Machine Theory*, 91, 120–134.
- Merlet, J. P., Gosselin, C. M., et al. (1998). Workspace of planar parallel manipulators. *Mechanism and Machine Theory*, 33(1–2), 7–20.
- Patterson, T., & Lipkin, H. (1993a). Structure of robot compliance. *Transactions of the ASME*, 115, 576–580.
- Patterson, T., & Lipkin, H. (1993b). A classification of robot compliance. *Journal of Mechanical Design*, 115(3), 581–584.
- Wu, J., Wang, J., Wang, L., & You, Z. (2010). Performance comparison of three planar 3-DOF parallel manipulators with 4-RRR, 3-RRR and 2-RRR structures. *Mechatronics*, 20(4), 510–517.
- Zhao, T., Zhao, Y., & Shi, L. (2007). Stiffness characteristics and kinematics analysis of parallel 3-DOF mechanism with flexible joints. In *The Proceeding of the IEEE International Conference on Mechatronics and Automation*, pp. 1822–1827.

Mechatronics and Robotics Engineering for Advanced
and Intelligent Manufacturing

Zhang, D.; Wei, B. (Eds.)

2017, X, 468 p. 240 illus., 173 illus. in color., Hardcover

ISBN: 978-3-319-33580-3